Building and Environment 243 (2023) 110731

Contents lists available at ScienceDirect

Building and Environment

journal homepage: www.elsevier.com/locate/buildenv

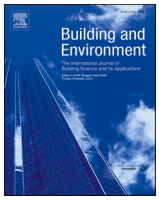

Climate adaptive urban measures in Mediterranean areas: Thermal effectiveness of an advanced multilayer green roof installed in Palermo (Italy)

Dario Pumo *, Francesco Alongi, Marcella Cannarozzo, Leonardo V. Noto

Dipartimento di Ingegneria - Università degli Studi di Palermo, Viale delle Scienze, Ed. 8, 90128, Palermo, Italy

ARTICLE INFO

Keywords:
Green roof
Climate change
Urbanization
Green infrastructure
Nature based solution
Urban heat island
Building thermal insulation

ABSTRACT

Several nature based and climate adaptive solutions have been proposed to improve cities resilience to the effects of global warming and restore natural processes in strongly anthropized areas. Green roofs are among the most efficient nature based solutions to address recurrent urban challenges, such as pluvial floods and urban heat islands. Various benefits offered by green roofs are rather known, such as their capacity to enhance buildings thermal insulation; green roofs also favor urban biodiversity, improving buildings aesthetic value and human well being. Multilayer green roofs (MGRs) are green roofs with an additional layer that increases their water storage capacity. Deep analyses on MGRs are still lacking due to their recent development, and the few works in literature are prevalently focused on their stormwater retention primary function. This work explores the thermal function of an experimental MGR prototype installed in Palermo (Italy), comparing its response to local climate with that of an unaltered portion of the rooftop through the analysis of surface temperature time series collected over a two years monitoring period. Performances are evaluated thought various daily thermal indices, also analyzing the role of the water stored into the system. Results contribute to raise awareness about the benefits arising from the use of MGRs in semi-arid Mediterranean urban areas, confirming, as main thermal advantage, their cooling effect, with mean daily surface temperature reduced by 8.4% outdoor and 5.8% indoor; performances increases with water storage and are particularly evident during the hot and dry summers that typically characterize such regions.

1. Introduction

Climate change and urbanization are profoundly modifying the atmospheric energy balance [1] and many of the processes involved in the hydrological cycle [2,3], with important fallouts on several environmental and socio-economic aspects (e.g. Refs. [4,5]). The population and extent of cities continue to grow [6] and this implies an increasing demand for water, energy, construction materials, and food [7] and new challenges for the scientific community and policy makers.

Climate change is causing heating and frequent heat waves, that are particular evident in urban areas. Urban surfaces typically have low albedo and high solar absorptance, and urban geometry could influence shade conditions and create urban canyons where the solar short-wave (SW) radiation, after multiple reflections between urban surfaces, can be trapped, absorbed by building walls and re-radiated as long-wave (LW) radiation. The reduced sky view factors could partially limit the LW radiation released outside the urban areas. Urban canyons might also impede cooling processes during the nighttime. The increasing temperature due to climate change and urbanization, as well as the anthropogenic heat produced by human activities in high density urbanized areas, are in fact the main causes of the well-known Urban Heat Island (UHI) effect, generating elevated temperatures at urban nuclei compared to the outlying rural areas [8]. UHI is becoming an important matter today, since it could further exacerbate the economic impacts of heat waves and represents an environmental stressor causing serious risks to human health and related social costs [9].

Moreover, high air temperatures can modify the distribution of pollutants in the air [10,11] and increase intensity and frequency of rainfall extremes [12,13]. Ground impacts of rainfall extremes are further exacerbated by urban expansion at the expense of green areas,

* Corresponding author.
E-mail addresses: dario.pumo@unipa.it (D. Pumo), francesco.alongi01@unipa.it (F. Alongi), marcella.cannarozzo@unipa.it (M. Cannarozzo), leonardo.noto@unipa.it (L.V. Noto).

https://doi.org/10.1016/j.buildenv.2023.110731
Received 22 June 2023; Received in revised form 11 August 2023; Accepted 12 August 2023
Available online 13 August 2023

causing frequent severe stress to the urban drainage systems.

Several researcher carried out specific studies (e.g. Refs. [14,15]), aimed to demonstrate the advantages that could arise from the implementation in urban areas of the so-called Nature-Based Solutions (NBSs). NBSs are "green" infrastructures inspired and supported by nature that include a series of sustainable and low-cost solutions aimed to restore pre-development conditions. NBSs, given their multipurpose nature [16], are ideal solutions to achieve many of the Development Goals (SDGs) proposed in the Sustainable Agenda 2030 [17].

Green Roofs (GRs) are climate adaptive NBS particularly appreciated by the society, since they allow to exploit otherwise unutilized spaces and offer a series of aesthetical as well as environmental, social and economic advantages [18,19]. Incorporating vegetation, growth medium and other landscape components on the rooftop of buildings provides several direct and indirect benefits, such as: i) stormwater attenuation [20] and heat stress mitigation [21], with possible potable water and energy consumption reduction; ii) water quality enhancement, since green roofs may buffer acidic rain and retain pollutants [22]; iii) attenuation of noise levels in urban spaces arising from road, rail and air traffic; iv) mitigation of air pollution, by directly consuming gaseous pollutants through vegetation or indirectly, by modifying microclimates [23]; v) restoring of biodiversity lost due to urban development, offering a safe recovery place for birds and insects; vi) extending of rooftop life, since GRs protect roof membrane from extreme heat, wind and ultra-violet radiation [24]; vii) providing social benefits including creation of educational and employment opportunities, recreational green areas and potential spaces for biological food production [25], with a series of positive implications for public health [26–28].

Green roofs have been traditionally used as thermal insulation measures for buildings. Actually, several experimental studies demonstrated how GRs are able to contribute to roof insulation of buildings, absorbing 60% of the direct solar radiation and reflecting about 20–30% [29], reducing daily temperature fluctuations, and consequently allowing energy to be saved from the air conditioning systems (e.g., Refs. [30–32]. In Mediterranean areas, thermal effectiveness of extensive, semi-intensive and intensive GRs was investigated in Portugal by Ref. [33]; showing that GRs enable up to 20% of energy saving for extensive solutions and up to 70% for intensive ones.

Several studies have been recently focused on the potentialities of GRs under different perspectives and at different scales, ranging from plot-scale, homes, buildings, and district levels (e.g., Refs. [34–36]). The direct monitoring and the identification of appropriate performances indicators, as well as the development of accurate methods and models to assess the response of such systems to past, present and future climate forcings, are essential aspects that might drive us toward the identification of new GRs design criteria oriented to the concepts of "design with nature", "resilience paradigm" and "building sustainability".

This work contributes to the understanding and quantitative assessment of some potential thermal benefits related to the use in a Mediterranean climatic area of a new typology of GRs, that is the so-called Multilayer Green Roof (MGR). The Mediterranean basin, which can be considered as a hot spot for climate change [37,38], urgently needs a big effort to promote and implement climate adaptive solutions such as GRs. Compared to traditional GRs, MGRs have a further "blue" layer for water storage, which allows for water retention and possible reuse, with a storage capacity comparable to that typical of Rainfall Harvesting Systems [18], such as blue roofs. In MGRs, the blue layer is connected to the upper "green" layer via capillary cones that allow for passive irrigation, supporting physiologic activities of the plants and reducing water stress during the driest periods. Due to their recent diffusion, potential advantages of MGRs are much less explored compared to traditional GRs [39]. Most of the scientific literature was focused on the main advantage that typically MGRs can provide, namely the ability to slow down and reduce stormwater volume in urban areas, due to their augmented water storage capacity with respect to traditional GRs [40,41]. Observational analyses to assess possible co-benefits of MGRs are still rather rare, especially in warm-temperate climates.

The analysis presented here is based on an experimental system installed in 2019 in Palermo (Italy), fully described in Sect. 2. The system could be assimilated to an extensive GR, considering its lightness and the limited thickness of the soil layer, and it has been monitored by a complex network of sensors, also described in Sect. 2, since December 2020, also monitoring an equal size portion of the rooftop bordering the system, used as benchmark "grey" roof for comparison.

The present research integrates a previous work [42], where the hydrological effectiveness of the experimental site was deeply evaluated, demonstrating from the analysis of the first year of monitoring, the high performance of the system in terms of retention capacity at rainfall event scale. The new analysis presented in this paper focuses on the thermal response of the system, exploring possible advantages of MGRs in terms of thermal insulation capacity and roof thermal inertia.

Different daily performance indices, defined in Sect. 2, are used and they are based on the comparison among air and roof surface temperature data measured at both outdoor and indoor sensors placed at the MGR and the benchmark grey roof. Such indices are analyzed at the level of entire two-year monitoring period and at the seasonal level, and the results are described in Sect. 3. A discussion on the main outcomes of the present study and their possible implications is reported in Sect. 4, while some concluding remarks conclude the paper.

Some aspects extremely innovative and specific for multilayer green roofs are treated, such as an analysis on the influence of the water storage on the thermal response of the system. Thermal benefits for MGRs are rarely quantitatively supported by field measures; sharing this type of information is fundamental for the development of reliable models able to reproduce the thermal response of MGRs to different climate forcings, which are key tools for various possible specific applications, such as extending the analysis from the plot scale to larger scales, or evaluating the potentialities under future scenarios impacted by climate change.

2. Materials and methods

2.1. Experimental site: the Polder Roof system

Multilayer-Green Roofs (MGRs) are characterized by the presence of a high-capacity storage layer, often referred to as blue layer (BL), located in the bottom part of the system. Rainwater is infiltrated into the upper green layer (GL), where it feeds the growing medium soil moisture useful for the vegetation physiological activities; when field capacity is exceeded, percolation water is conveyed toward the lower BL where it is retained up to the fulfillment of the storage retention capacity; water exceeding the BL retention capacity is finally released out of the system as outflow discharge.

Water volume retained by the system is extremely important, since it can reduce the pressure on urban drainage systems during intense storms, and represents, at the same time, a useful water resource for possible non-potable reuses (e.g., flushing toilets and clothes washing, car washing and garden irrigation) and passive irrigation of the same system vegetation. Water storage and system outflow can be controlled dynamically through a retention control weir, which in advanced systems such as that considered for this paper, can be regulated remotely and automatically according to predefined targets [42].

The hydrological and thermal efficiency of MGRs strongly depends on the properties of the system, such as the GL and BL depth, the type of substrate and vegetation, the retention control weir management [42]. also demonstrated how the retention rate of MGRs relies on the system initial conditions, in terms of GL soil moisture content and BL water storage immediately before the rainfall occurrence, and the characteristics of the incoming rainfall (i.e., total amount, intensity, duration).

The experimental site under analysis (Fig. 1a), called Polder Roof was developed by the Dutch company Metro-Polder and installed in June 2019 within the project *Polder Roof Field Lab*, supported by the

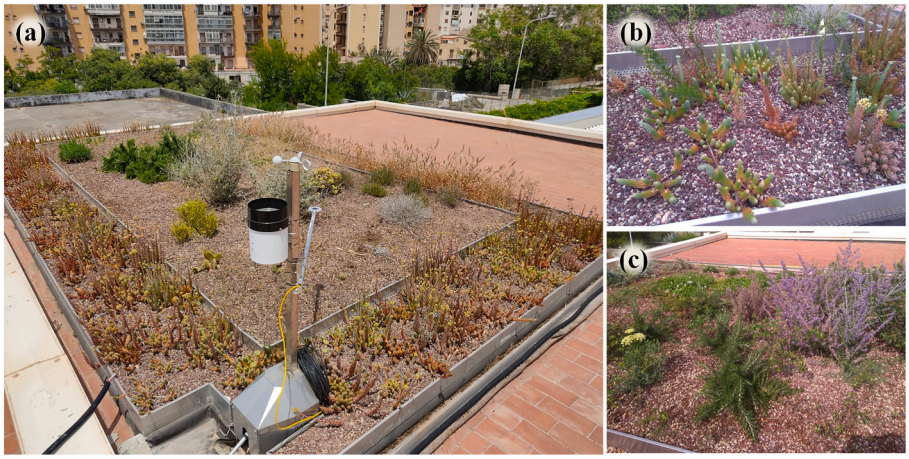

Fig. 1. (a) Experimental site after about 3 years from installation (Aug 2022); (b) sedum species in the shallower region (Apr 2022); (c) shrub and aromatic species in the deeper region (Apr 2022).

European Institute of Innovation and Technology (EIT) Climate-KIC (*Knowledge and Innovation Community*) program. Other three similar prototypes have been also installed within the same project in the Italian cities of Cagliari, Perugia and Viterbo, and are described in Ref. [43].

The installation covers a rectangular portion of 32.1 m^2 of the rooftop of the Engineering Department of the University of Palermo (Italy). An equal size area adjacent to the MGR, hereafter referred to as "grey roof" (GrR), is used as reference unaltered roof surface for comparison. Two sub-regions can be distinguished: a central sub-region of 18,0 m^2 with soil depth of 20 cm and a border sub-region of 14,1 m^2 with soil depth of 10 cm. Soil constituent materials meet the requirements of the Italian standard UNI 11235 (2015). In particular, the substrate for both the sub-regions is made of a fertile and extremely light soil consisting of a mixture of volcanic lapillus (90%) and pumice (10%). Vegetation is composed by a selection of typical autochthonous species for Sicily, rather drought-tolerant once established and selected in order to favor their adaptability with respect to local climate. The shallower sub-region (Fig. 1b) has been realized by various sedum species, and typical Mediterranean meadow species while the deeper sub-region (Fig. 1c) is covered by different perennial and aromatic species.

The GL is supported by the BL and separated from this by a capillary geotextile drainage membrane. The BL is a 10 cm height water retention box consisting of a modular system produced by the Permavoid Company (http://www.permavoid.co.uk/) that combines plastic support units, enabling stormwater storage and conveyance, with capillary columns, enabling natural capillary irrigation. The system is completed by a protective geotextile filter fabric and a waterproof membrane.

2.2. Monitored variables

The MGR is equipped with its own integrated monitoring system, named SmˆrtMILL, which includes a set of sensors for rainfall, temperature, and water height into the BL; SmˆrtMILL collects data with 10 min frequency, and transmits them to a Metro-Polder dashboard accessible on the internet, called AQORA. A dynamic control of the water storage into the BL and outflow discharge release is operated by a semi-automatic outflow control system, called Smart Flow Control (SFC), by which the control weir can be remotely regulated at any time from the dashboard or programmed, setting opening degrees and timing. During the entire period of monitoring, the weir was set constantly at the maximum closure corresponding to a height of 7 cm.

Besides the SmˆrtMILL system, the MGR and the GrR are monitored by an external weather monitoring station, a system of two rain barrels equipped with water depth sensors and a set of thermometers. The weather station is located in close proximity (i.e. 65 m) to the experimental site and it is equipped with three different sensors for rainfall monitoring and a meteorological weather station, both transmitting data to a local server. Rainfall is monitored, with 1 min data acquisition frequency, by a weighing rain gauge (OTT Pluvio2-400), a laser-optic disdrometer (OTT- Parsivel2) and a tipping bucket rain gauge (LSI LASTEM - DQA130.1). The weather station is equipped with a thermo-hygrometer (Lambrecht 8096) and an air pressure sensor (Lambrecht 8128). More detailed information about such sensors can be found in Ref. [44]. All data from the weather station are published online at the HYCLIC (*HYdrology & Climate change ImpaCts Lab*) website (http://idrologia.unipa.it/) and freely available on request.

A system of two external plastic rain barrels with a capacity of 1000 l receives separately discharge outflows from the MGR and the GrR; each rain barrel is equipped with a couple of pressure sensors (i.e., vanEssen micro-diver and baro-diver barometric pressure loggers), which allows for measuring, with 5 min acquisition frequency, water levels and, consequentially, volumes released from the two different portions of the roof.

Roof surface temperatures are measured with 30 min acquisition frequency by a set of four thermometers (MX2203 by HOBO); more specifically, two couples of sensors are installed at vertical corresponding positions in the upper (outdoor) and bottom (indoor) surface of both the MGR and the GrR. Outdoor sensor for the MGR was installed at depth of about 5 cm below the soil surface, in the central point of the system, while the other outdoor sensor was placed on the central point of the external GrR roof surface. Indoor sensors for both the MGR and the GrR are installed on the ceil of two separated, conterminous, not air-conditioned and scarcely utilized rooms, where the presence of a secondary modular ceiling system, placed 33 cm below the roof, minimizes the effects of potential different thermal and ventilation conditions in the two rooms. The two rooms have equal surface (34.1 m^2) and height (4.1 m), and both have an equal size (3.0 × 1.6 m), permanently locked, window facing north-west.

2.3. Local climate in Palermo

Palermo is the fifth most populated city in Italy. It lies on Sicily's northwestern coast at the head of the Bay of Palermo, facing east. Inland the city is enclosed by a large plain and the surrounding mountains that rise up to an elevation of about 1.000 m a.s.l north of the city. Local climate is classified as *Csa - Hot-summer subtropical Mediterranean climate* according to the Köppen-Geiger climate classification, with long, hot and dry summers and rainy winters. A characterization of rainfall and temperature regime of the city based on the analysis of the last two decades (2002–2022) of data collected at the gauge station ID 276-

Uditore of the SIAS (*Servizio Informativo Agrometeorologico Siciliano*) regional agency, about 3 km far from the experimental site, is reported in Fig. 2, from which it can be observed a mean annual air temperature of 18.9 °C, with mean daily values around 26.2 °C during the summer and 12.4 °C during the winter. The hottest month is August (mean daily temperature 27.2 °C), while the coldest one is January (mean daily temperature 11.9 °C). The daily temperature excursion is rather relevant (mean equal to 7.4 °C and maximum of 20.3 °C), with low temperature during the night due the heat exchange and the thermal inversion, and with temperature during the diurnal hours that can reach very high value, especially during the summer, under non-windy conditions (maximum record 44.2 °C in June 2007).

The mean annual precipitation is 740 mm, with on average 554 mm (75%) during autumn and winter. The mean monthly precipitation spans from about 13 mm/month (in June, July and August) to about 97 mm (for the months from October to January). Rainfall retention measures are particularly useful in Palermo, which is periodically affected by urban pluvial floods with significant economic damages [45].

2.4. Dataset and performance indices

In this study, a two-years reference period, from Dec. 22nd, 2020 to Dec. 31st, 2022, is analyzed. Rainfall series was obtained using data from the weighing pluviometer, that among the various sensors is the one offering the highest accuracy. Some missing data (1.7% in total) have been filled with data from the disdrometer and the tipping-bucket gauge. Besides the daily rainfall depth (P in mm), the weather at each day is also characterized by the mean daily air temperature (T_{air} in °C) measured by the weather station.

The two monitored years, especially 2022, were characterized by less rain (on average 684 mm/year) and higher temperature (on average 19.6 °C) compared to the long period averages for Palermo (Fig. 2). Fig. 3 shows the frequency histograms of P (left) and T_{air} (right) over the monitoring period, distinguishing in this last the histogram relative to only rainy days (blue bars) and that relative to no-rainy days (red bars). It can be noticed how most of the significant (i.e., $P > 2$ mm) rainy days (i.e. 106 out of a total of 121 rainy days) were characterized by light/moderate daily rainfall depth, i.e. lower than 20 mm according to the [46] classification. Moreover, rainy days are characterized by low temperature, since they are mainly concentrated during the coldest winter/spring seasons.

The system antecedent conditions are evaluated through indices derived from literature [42,47–49] and slightly modified for the purposes of our analysis, with the objective of assess the amount of water present within the different layers of the system at the day of evaluation. The adopted indices (Table 1) are: i) the Antecedent Dry Weather Period (ADWP), given by the number of days to the last rainy day before the day of evaluation; ii) the Degree of Water Storage (DWS), given by the percent ratio between the mean daily water level into the BL at the day of evaluation and the thickness of the BL (i.e. 10 cm); iii) the 5-days Antecedent Precipitation Index (API_5), here defined as the cumulative precipitation over the last 5 days, including the day of evaluation; iv) the 5-days Antecedent Temperature Index (ATI_5), given by the mean daily temperature over the last 5 days, including the day of evaluation; and v) the 5-days Antecedent Runoff Index (ARI_5), equal to the cumulative runoff produced by the MGR in the last 5 days, including the day of evaluation. Due to a sensor malfunction, data of BL water levels are available only from Jan. 15th, 2021 to Jun. 29th, 2021, and thus the DWS has been calculated only over a short initial time window of the monitoring period.

The analysis of thermal benefits has been carried out on 30-min temperature time series recorded by the four surface thermometers (outdoor/indoor sensors at the MGR and the GrR) and air temperature time series measured by the weather station, computing the thermal indices defined in Table 1. Original temperature time series present very few missing data: 97 for the outdoor GrR sensor, 9 for each of the other three surface temperature sensors, and 14 for the air temperature sensor, on a total of 35,520 data per series. Daily temperature data, arising from time aggregation of 30-min data with more than 13% of missing data per day (i.e. more than 3 h per day) have been excluded from the analysis, leading to a total of only three daily data removed from the outdoor GrR sensor (i.e. a period from 22 to 24 Feb. 2020 during which the sensor was under maintenance).

Surface Temperature Reduction (STR), External Temperature Ratio (ETR) and Temperature Excursion Reduction (TER) reported in Table 1 are typical indices of literature [31,50]; the first compares the average daily surface temperature at the MGR with that measured at the GrR, with regard to both indoor (STR_{in}) and outdoor (STR_{out}) sensors. The External Temperature Ratios (ETR_{max} and ETR_{min}) are given by ratio between the maximum (or minimum) daily surface temperature from the outdoor sensor and the maximum (or minimum) daily air temperature, and they are computed separately for both the MGR and the GrR.

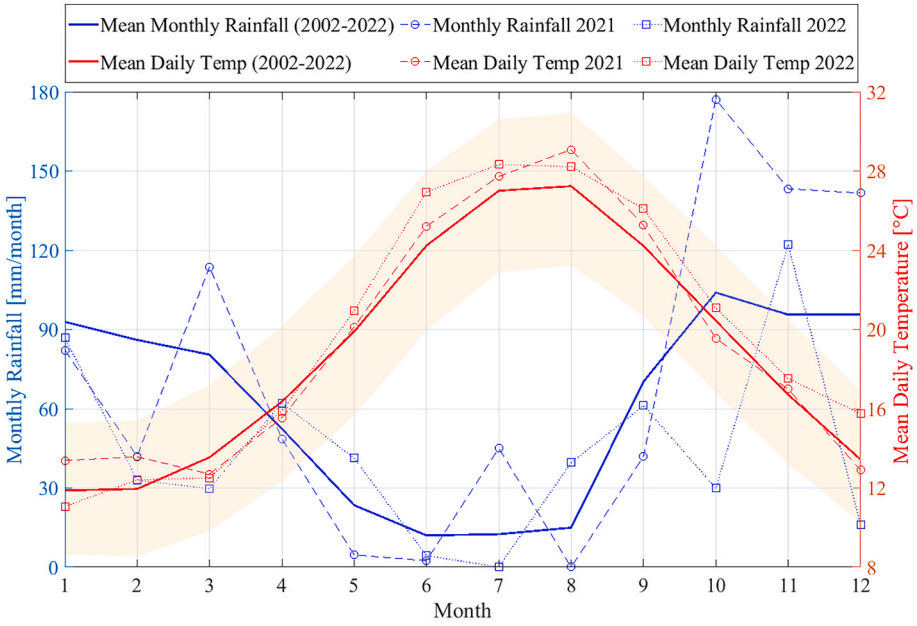

Fig. 2. Climate in Palermo (data from the SIAS gauge station ID 276-Uditore: 2002–2022): mean monthly rainfall (mm/month, blue solid line), mean daily temperature (°C, red solid line) and its monthly variation range (shadowed area). Dashed lines refer to data of rainfall (blue) and temperature (red) collected at the experimental site during 2021 (circles) and 2022 (squares). (For interpretation of the references to color in this figure legend, the reader is referred to the Web version of this article.)

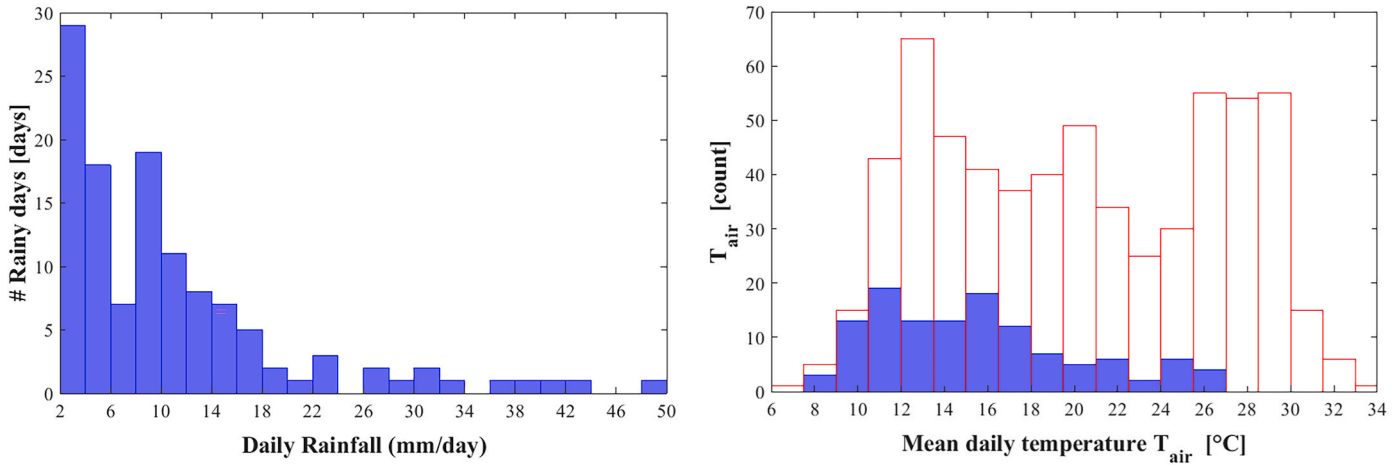

Fig. 3. Monitoring period: from Dec. 22nd, 2020, to Dec. 31st, 2022. Frequency histograms of daily rainfall depth (left plot) and mean daily air temperature (T_{air}, right plot). Blue color refers to rainy days, while red refers to no-rainy days. (For interpretation of the references to color in this figure legend, the reader is referred to the Web version of this article.)

TER index refers to the daily surface temperature excursion (T_{exc}), given by the difference between the maximum and the minimum roof surface temperature measured in a day; more specifically, TER compares MGR and GrR roof temperature excursions, and it is computed considering both the indoor (TER_{in}) and the outdoor (TER_{out}) data.

3. Results

3.1. Temperature comparison at the MGR and the GrR

Green roofs are known to be capable of reducing roof surface temperature and daily temperature excursion compared to grey roofs [21]. At equal substrate depth, MGRs in a semiarid environment are expected to further improve building thermal insulation, especially during hot summer conditions, due to the presence of a further insulation layer filled by air and water with a dynamic ratio. The mean daily temperature and the daily temperature excursion over the entire reference period measured on the roof surface by the MGR and GrR sensors are reported in Fig. 4, where they are also compared with the mean daily air temperature measured by the weather station (red line). Upper graph refers to the outdoor sensors, while bottom graph to the indoor sensors. As it clearly appears from the upper graph, the outdoor GrR average surface temperature follows approximately the average air temperature during the colder months of the year, while it is on average sensibly higher than air temperature during the hotter summer months; moreover it is characterized by a pronounced daily excursion, highlighted by grey shadow area, especially during the summer where it reached almost 32 °C. The overall effect of the MGR was to reduce the outdoor surface temperature (on average −1.8 C° over the entire monitoring period compared to the GrR), especially during the summer season (on average −2.8 °C) where in some days of August the outdoor average surface temperature of the GrR was also over 8 °C higher than in the MGR. The decay of the daily thermal excursions in the vegetated roof, highlighted by green shadow area, compared to the unaltered roof is even more evident; the mean daily excursion recorded at the outdoor MGR sensor was equal to 2.9 °C (vs. 21.4 °C for the GrR), while the maximum values, occurring at the end of the spring when the differences between diurnal and nocturnal temperatures are usually more relevant, were around 8.8 °C for the MGR (vs. 31.7 °C for the GrR). This effect can be interpreted as clear evidence of the increased thermal inertia due the MGR presence.

The analysis of indoor temperature in the bottom graph of Fig. 4 shows how the mean daily MGR surface temperature (20.5 °C) over the entire reference period is lower than the mean daily GrR surface temperature (21.8 °C), approaching the mean air temperature value (19.5 °C). Nevertheless, it can be noticed how the maximum daily surface temperature at the MGR indoor sensor exceeds 32 °C in only 33 days out 740, with maximum value equals to 32.8 °C, while at the GrR indoor sensor this value was overcome in 123 days, with a maximum of 35.1 °C.

Mean seasonal values and mean values over the entire period of the minimum, average and maximum daily temperature recorded at the four surface temperature sensors and at the weather station are summarized in Table 2, where it can be noticed how, as it was expected, on average the minimum daily temperature at the MGR outdoor sensor is always relevantly higher than that at the GrR outdoor sensor, especially during the spring (+6.6 °C) and, at the same time, the maximum temperature at the MGR outdoor surface is always relevantly lower than those at the GrR outdoor sensor, especially during the hottest season of the year, i.e. the summer (-15.2 °C). The indoor MGR surface is always colder than the indoor GrR surface, especially during the spring, with reductions in terms of maximum temperature higher than for the mean and the minimum daily temperature, leading to an overall reduction by the 30% of the daily temperature excursion for the MGR compared to the GrR.

Fig. 5 shows a comparison between the daily surface temperature profiles for the “mean day” of the four seasons. Each profile is derived averaging all the data recorded during a given season by a given sensor, according to the original 30-min time-resolution of acquisition. In each graph, the corresponding mean daily air temperature profile is also reported.

From the analysis of the left plots of Fig. 5 referring to the outdoor sensors, it can be observed how, for all the seasons, the GrR surface temperature follows the average solar irradiance daily profile, with roof surface colder than the air temperature during the night, and relevantly hotter during the daylight hours. The MGR shows an inverse behavior, with surface temperature higher than air temperature during the night, especially during the hottest spring/summer seasons, and lower during the hottest daylight hours, especially during the coldest autumn/winter seasons, reaching, for all the seasons, a minimum around noon and a maximum approximately 2 h after the sunset.

This behavior could be explained by the fact that the MGR outdoor sensor is installed 5 cm below the GL surface and soil-vegetation systems are typically characterized by higher albedo and thermal inertia compared to conventional rooftop paving systems [51], which implies an attenuation of the solar irradiation thermal loads and temperatures daily variability, respectively. This, together with the augmented thermal insulation due to the presence of an extra layer with respect to the GrR, also explains the differences between the mean daily profiles of the

Table 1
Monitored variables and indices (temp. = temperature; surf. = surface; BL= Blue Layer).

		Symbol	Unit	Definition
System Antecedent Conditions	*Antecedent Dry Weather Period*	**ADWP**	*day*	Time to the last rainy day before the day of evaluation
	Initial Degree of Water Storage	**IDWS**	*%*	Percent ratio between the mean daily BL water and the BL thickness (10 cm)
	Antecedent Precipitation Index	**API_5**	*mm*	Cumulative precipitation over the last 5 days, including the day of evaluation
	Antecedent Temperature Index	**ATI_5**	*°C*	Mean daily temperature over the last 5 days, including the day of evaluation
	Antecedent Runoff Index	**ARI_5**	*mm*	Cumulative outflow from the MGR over the last 5 days, including the day of evaluation
Rainfall	*Daily Rainfall Depth*	**P**	*mm*	Total amount of daily rainfall
Temperature	*Air Temperature*	**T_{air}**	*°C*	Air temp. from the weather station
	Outdoor MGR Temperature	**$T_{out,MGR}$**	*°C*	Outdoor temp. on the external surface of the MGR
	Outdoor GrR Temperature	**$T_{out,GrR}$**	*°C*	Outdoor temp. on the external surface of the GrR
	Indoor MGR Temperature	**$T_{in,MGR}$**	*°C*	Indoor temp. on the internal surface of the MGR
	Indoor GrR Temperature	**$T_{in,GrR}$**	*°C*	Indoor temp. on the internal surface of the GrR
	Daily Temperature Excursion	**T_{exc}**	*°C*	Difference between max and min daily temp.
Thermal Indices	*Surface Temperature Reduction*	**STR**	-	= (Indoor/Outdoor) MGR/(Indoor/Outdoor) GrR mean daily surf. temp.
	External Temperature Ratio	**ETR**	-	= (MGR/GrR) Outdoor surf. (Min/Max) daily temp./Air (Min/Max) daily temp.
	Temperature Excursion Reduction	**TER**	-	= (Indoor/Outdoor) MGR/(Indoor/Outdoor) GrR daily temp. excursion

indoor roof surface temperature for the MGR and the GrR, shown in the right plots of Fig. 5. For all the seasons, the two profiles for the MGR and the GrR appear almost specular, with the former laying lower than the latter, except for 3 h in autumn, especially during the spring and summer seasons, when differences in the mean temperature of some night hours reached values over 2 °C. Differently from the GrR profiles, in the MGR, the shape of the indoor mean daily surface temperature profiles follows that of the corresponding outdoor profiles, even if with much less marked hourly temperature fluctuations; the maximum temperature excursion from the indoor mean daily profile of the MGR is about 0.8 °C, occurring in spring and summer, while it reaches 4.6 °C during the summer for the outdoor profile.

As it emerges from Fig. 5 and Table 2 and in winter months, MGR showed outdoor/indoor maximum surface temperatures markedly lower than the GrR. Indeed, in winter, the elevated absorption coefficient of the reference surface can generate significant heat gain through the roof cover, which may eventually lead to mean daily surface temperature for the GrR higher than for the MGR. With specific regard to the thermal comfort for internal spaces, this could appear as a possible disadvantage of the MGR since, during the winter, roof surfaces are frequently below the internal comfort temperature, and, therefore, a lower surface temperature for the MGR could further exacerbate potential thermal discomfort. However, this is partially compensated by the lower temperatures occurred during nighttime at the GrR because of the intense heat exchange with the sky; this aspect explains why indoor mean daily temperatures at the MGR are not so dramatically distant from the reference roof during the winter. Moreover, the gain in terms of thermal insulation for the MGR, demonstrated by the significant reduction of the daily temperature excursion also during the winter, limits negative heat fluxes from indoor spaces to the outdoor environment; this favors a slower thermal dispersion with a more stable internal air temperature, which implies a potential lower effort and energy consumption for heating internal spaces.

3.2. Evaluation of the thermal performances

The quantitative evaluation of the thermal benefits of the MGR is here performed through the computation of the indices listed in Table 1; the results, in terms of daily indices over the entire period and each season, are displayed as boxplots in Fig. 6. STR and TER indices (upper plots) provides an immediate comparison of the external/internal surfaces temperature between vegetated and unaltered roofs; red boxplots refer to indices computed using data from the outdoor sensors, while black boxplots are computed using data from those indoor. The STR values (top-left plots) for all the analyzed periods are prevalently lower than unit, denoting average daily surface temperature for the MGR lower than for the GrR for both outdoor and indoor roof surfaces. The outdoor indices behavior (red boxplot) derives from the fact that heat exchange between the sky and the GrR surfaces is more intense than for the MGR, since the absorptance of the concrete surfaces, measuring the effectiveness in absorbing radiant energy, is more elevated than for vegetated surfaces. This can generate a significant diurnal heat gain for the GrR outdoor surface, as it can be also noticed from the comparison among the outdoor temperature daily profiles in Fig. 5. The outdoor STR median value over the entire period is equal to 0.91, while it ranges from 0.85 in winter to 0.94 in autumn, with the lowest variability of the index during the summer (Inter-Quartile Range, IQR = 0.07) and the highest (IQR = 0.18) during the winter. The indoor STR boxplots (black boxplots in top-left panel of Fig. 6) confirm the well-known cooling effect of vegetated roofs. In this case, indices are less variable than outdoor STR values for all the seasons; the indoor STR median value over the entire period is equal to 0.94, and its seasonal value ranges from 0.91 in spring to 0.98 in autumn, with corresponding values of IQR about from one-quarter to one-half of the values referring to the outdoor STR, and the lowest and the highest variability again during the summer (IQR = 0.02) and the winter (IQR = 0.10), respectively.

ETR indices, shown in bottom plots of Fig. 6, provide a comparison between outdoor roof surface temperature and air temperature, considering both ETR_{min} and ETR_{max} daily values with green and blue boxplots for both indices referring to the MGR and the GrR, respectively. From the boxplots analysis, it is possible to notice that the ETR_{max} was constantly above the unit for the GrR and prevalently below one for MGR, while an opposite behavior can be observed with respect to the ETR_{min}. These results can be addressed to the fact that, on the one hand, the maximum values of the outdoor daily surface temperature for the conventional grey roof were constantly higher than air temperature maxima due to the marked influence of solar irradiance, and, on the other hand, the vegetated roof, especially during the colder seasons, could be also subjected to a cooling effect due to negative heat fluxes from indoor to outdoor spaces, which, as it can be observed from Fig. 5, could even nullify the diurnal heat gain due to solar irradiance in the MGR outdoor surfaces. Conversely, ETR_{min} prevalently below the unit for the GrR and above the unit for the MGR can be explained by the higher thermal insulation of the MGR compared to the GrR, which

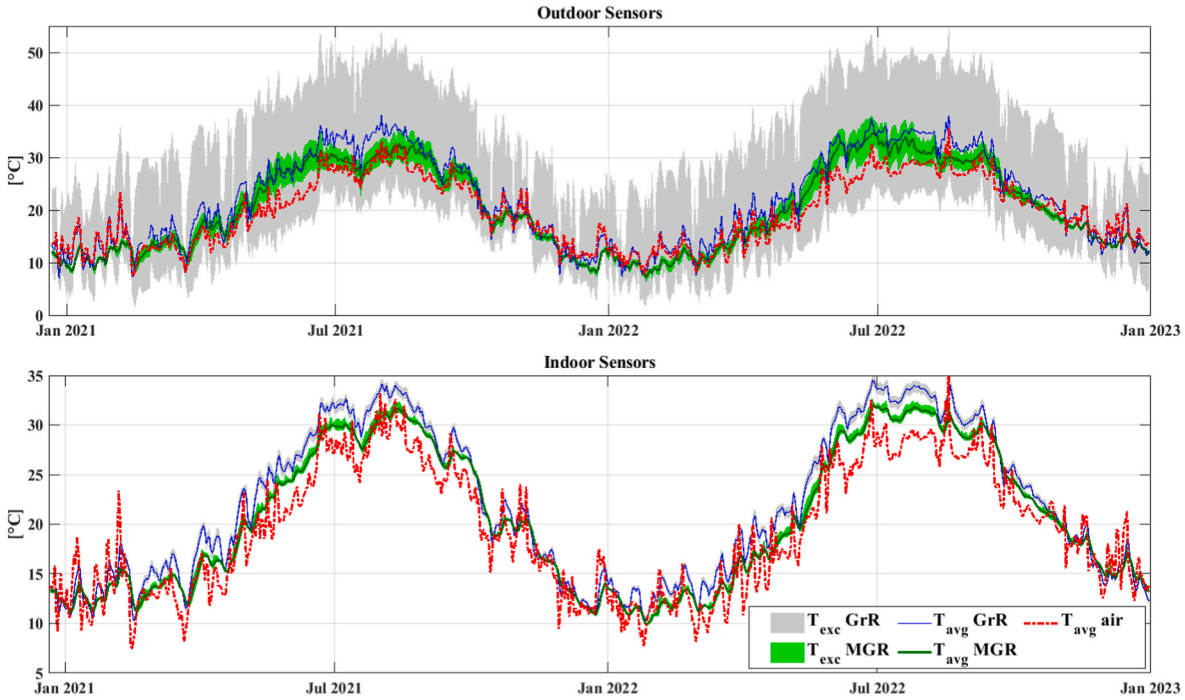

Fig. 4. Average daily roof surface temperature (T_{avg}) measured at the two pairs of outdoor (upper plot) and indoor (bottom plot) sensors of the MGR and the GrR. Daily temperature excursions (T_{exc}) for the MGR (green shadow area) and the GrR (grey shadow area) are also reported, as well as the average daily air temperature (red dashed line). (For interpretation of the references to color in this figure legend, the reader is referred to the Web version of this article.)

Table 2
Air temperature (T_{air}) and outdoor/indoor roof surface temperature for the MGR and the GrR. Mean seasonal values and mean over the entire monitoring period (FULL) for minimum (T_{min}, in italics), average (T_{avg}, in bold), maximum (T_{min}) daily temperature, and daily temperature excursion (T_{exc}, in bold italics) are reported in °C.

		AIR	OUTDOOR		INDOOR	
		T_{air}	$T_{out,MGR}$	$T_{out,GrR}$	$T_{in,MGR}$	$T_{in,GrR}$
FULL PERIOD	T_{min}	*15.9*	*18.8*	*13.8*	*20.2*	*21.3*
	T_{avg}	**19.5**	**20.2**	**22.1**	**20.5**	**21.8**
	T_{max}	23.1	21.8	35.2	21.0	22.4
	T_{exc}	***7.15***	***2.94***	***21.41***	***0.72***	***1.04***
WINTER	T_{min}	*9.6*	*10.4*	*6.6*	*12.5*	*13.3*
	T_{avg}	**12.7**	**11.2**	**12.9**	**12.7**	**13.6**
	T_{max}	16.2	11.9	24.6	13.0	14.1
	T_{exc}	***6.59***	***1.49***	***17.95***	***0.54***	***0.88***
SPRING	T_{min}	*15.0*	*20.0*	*13.4*	*20.2*	*22.0*
	T_{avg}	**19.0**	**22.0**	**23.7**	**20.5**	**22.5**
	T_{max}	22.7	24.2	37.9	21.2	23.3
	T_{exc}	***7.74***	***4.17***	***24.56***	***1.02***	***1.31***
SUMMER	T_{min}	*24.0*	*28.0*	*22.4*	*29.6*	*31.1*
	T_{avg}	**28.0**	**30.3**	**33.1**	**29.9**	**31.7**
	T_{max}	31.8	32.7	47.9	30.4	32.3
	T_{exc}	***7.77***	***4.65***	***25.52***	***0.86***	***1.20***
AUTUMN	T_{min}	*15.4*	*17.0*	*12.9*	*19.0*	*19.2*
	T_{avg}	**18.4**	**17.8**	**18.8**	**19.2**	**19.5**
	T_{max}	21.9	18.5	30.5	19.5	20.0
	T_{exc}	***6.50***	***1.48***	***17.64***	***0.47***	***0.80***

results less sensitive to the external air temperature; this implies a smoothing effect of the daily surface temperature excursion compared to the air temperature excursion that is more relevant for the MGR than for the GrR, with a minimum temperature at the vegetated surface significantly higher (on average + 5 °C) than at the grey surface.

Among the different indices, TER, shown in the top-right panel of Fig. 6, is probably the most indicative of the gain in terms of thermal insulation capacity and thermal inertia provided using MGRs; values lower than one denote a reduction in the daily excursion of surface temperature at the MGR compared to that at the GrR, which implies more stable temperatures during the day. Actually, at the indoor sensors (black boxplots) we found a median TER equal to 0.66 over the entire monitoring period, with median values for the hot and dry seasons equal to 0.77 and 0.73 for the spring and summer, respectively and higher than those relative to the wetter and colder seasons, which are equal to 0.53 and 0.55 for the autumn and winter, respectively, and characterized by a similar variability over the various seasons; this emphasizes the augmented capability in presence of the system to prevent heat loss from indoor spaces through the roof cover, especially during the colder months. TER values for the outdoor sensors (red boxplots) were much lower and less variable than indoor TER values. Again, the lowest TER median values were found during the colder seasons with values equal to 0.07 and 0.08 for the autumn and winter, respectively, while during the hotter seasons the medians were equal to 0.17 for both spring and summer. The seasonal IQR values of outdoor TER indices were, on average, one order of measure lower than those for the indoor TER. It is worth emphasizing that the daily outdoor TER never exceeded 0.54, which implies that the daily temperature excursion at the outdoor MGR surface was always more than halved compared to that relative to the outdoor surface of the unaltered grey roof. TER indices analysis highlights how the main thermal advantage of the use green roofs in Mediterranean semi-arid region is its capacity to attenuate the daily temperature fluctuations at the outdoor roof surfaces, whose combined effect with the augmented thermal insulation capacity and thermal inertia, eventually leads to a significant reduction also in the daily temperature excursion at the indoor surface of roof.

3.3. *Influence of stored water on the thermal response of the system*

Compared to traditional GRs, the water storage capacity of a MGR is higher and residence times of the water stored into the system, which depends on the operational rules of the control weir, are usually longer. In order to assess the role of water in determining the thermal response of the MGR to the external climate forcings, we analyzed the impact of the indices of system antecedent conditions defined in Table 1 on the

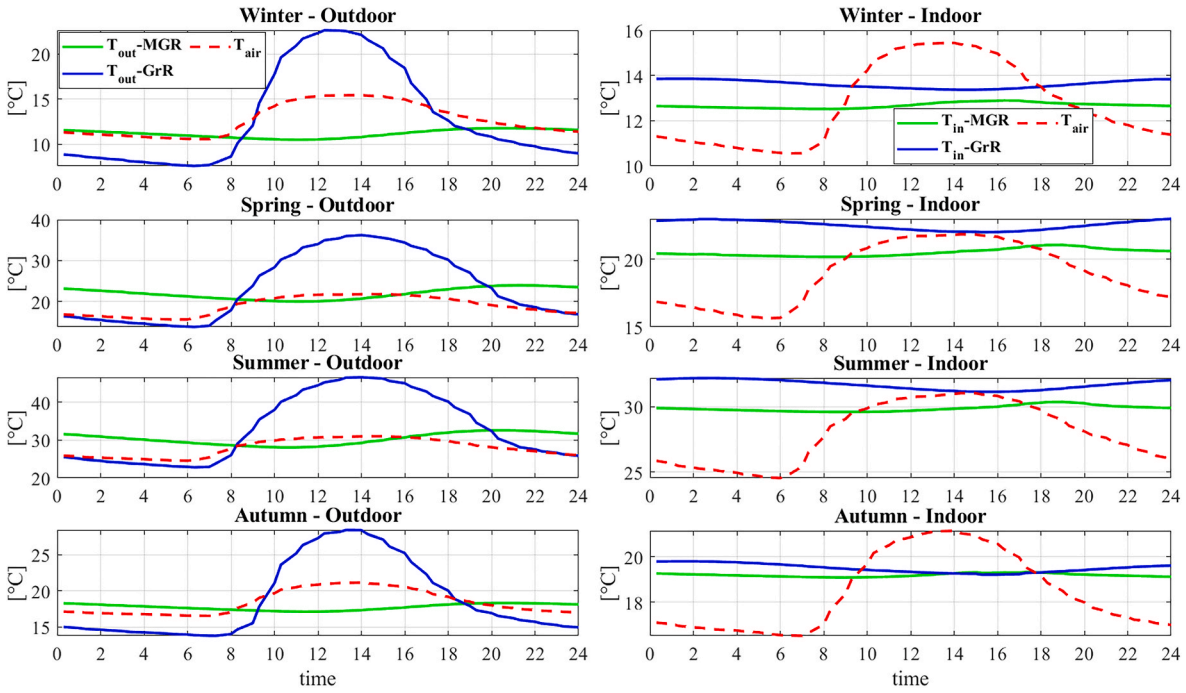

Fig. 5. Mean daily temperature profiles for the "mean day" of the four seasons. Each plot refers to the season indicated in the title and shows daily curves relative to mean values of the 30-min temperature records at outdoor (left plots) and indoor (right plots) sensors of the MGR (green) and the GrR (blue), and the corresponding mean daily air temperature profile (red dashed curves). (For interpretation of the references to color in this figure legend, the reader is referred to the Web version of this article.)

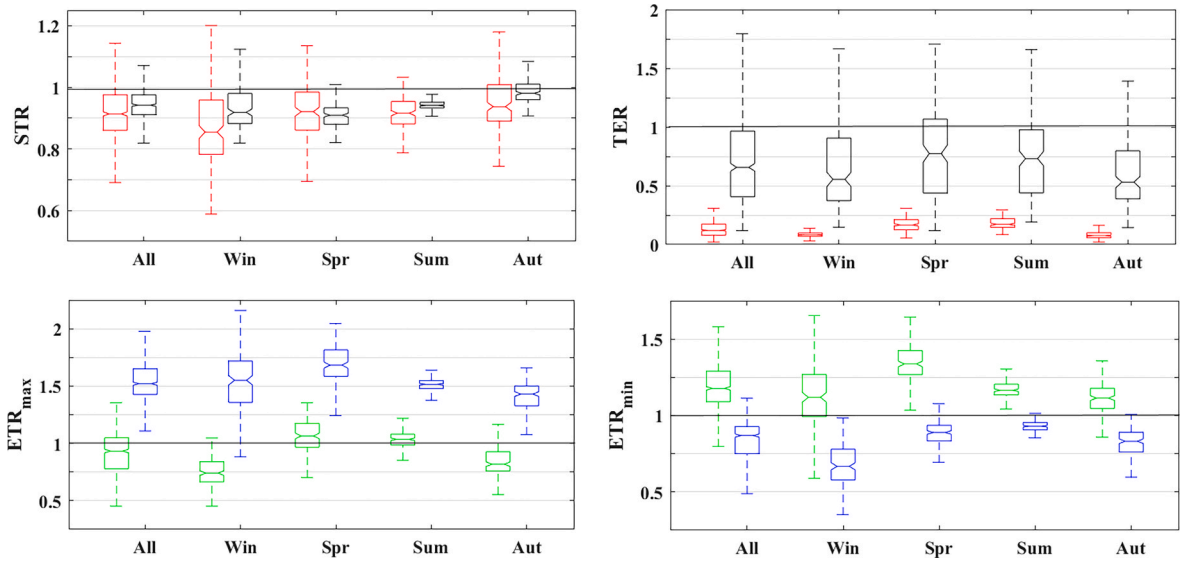

Fig. 6. Boxplots of the daily thermal indices defined in Table 1. Boxplots are computed over the entire period (All) and the four seasons. STR and TER are displayed in the upper plots, where boxplots referring to outdoor sensors are reported in red, while black boxplots refer to indoor sensors data. In the bottom plots, ETR derived using maximum (left) and minimum (right) daily temperature are reported separately; green and blue boxplots refer to indices computed using outdoor sensors data at the MGR and the GrR, respectively. Outliers are not displayed to help visualization. (For interpretation of the references to color in this figure legend, the reader is referred to the Web version of this article.)

STR and TER indices. Long ADWP values, usually greater than three-four weeks, depending on the season, are always associated to a null ARI_5, and indicative of almost absence of water in both GL and BL; on the contrary, not null ARI_5 values occur only when the BL has been filled up to its maximum retention capacity at least once in the previous 4 days or at the day of evaluation, and this, in turn, implies the overcoming of the field capacity in the GL triggering the percolation processes that feed the BL. Null API_5 associated to high ATI_5 could be representative of low soil moisture conditions in the GL, regardless to the BL degree of fullness.

Figs. 7 and 8 show scatter matrices relating paired thermal and antecedent condition indices. In particular, scatterplots with black points relates thermal indices with each other, scatter plots with red points relates thermal indices with antecedent condition indices, scatter plots with green points relates antecedent condition indices with each other, while bar plots provide frequency histograms for each one of the indices.

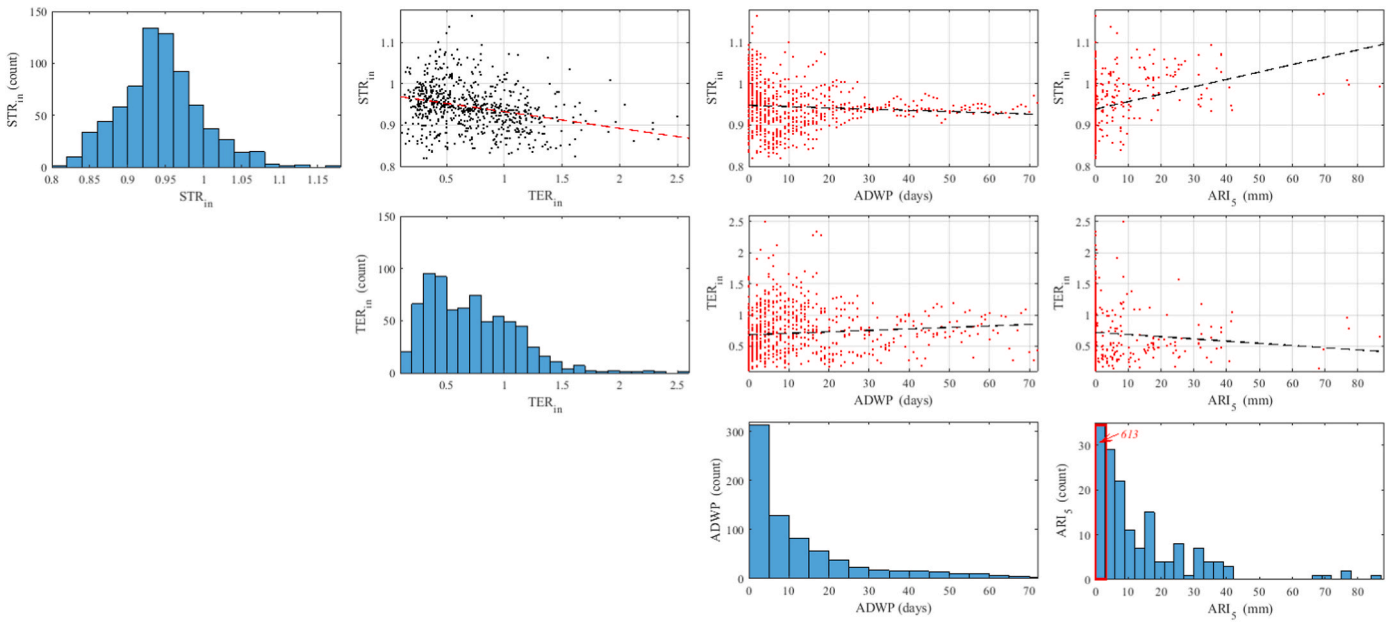

Fig. 7. Scatter matrix considering two thermal indices (STR_{in} and TER_{in}) and two antecedent condition indices (ADWP and ARI_5). Figure shows frequency histograms for all indices, and correlation plots, with the associated trend line, for all the possible pairs of indices, except for ARI_5 *vs.* ADWP, due to its scarce significance.

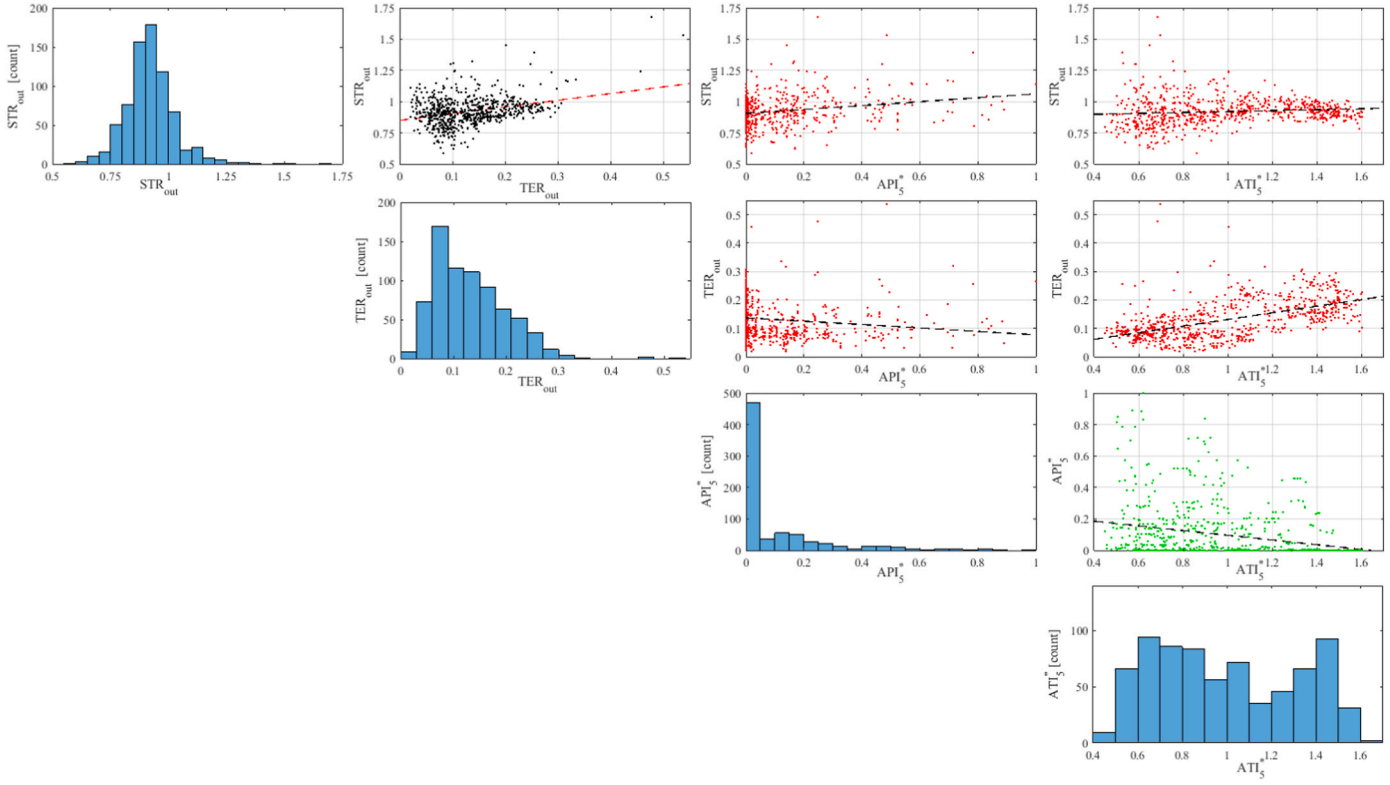

Fig. 8. Scatter matrix considering two thermal indices (STR_{out} and TER_{out}) and two antecedent condition normalized indices, API_5*and ATI_5*; the former is the API_5 normalized with respect to the maximum, while the latter is the ATI_5 normalized with respect to mean daily temperature over the reference period. Figure shows frequency histograms for all indices, and correlation plots, with the associated trend line, for all the possible pairs of indices.

Fig. 7 refers to the indoor STR and TER indices and the ADWP and ARI_5 indices. It can be noticed how, TER_{in} values show a clear decreasing trend with STR_{in}, assuming value above unit prevalently when STR_{in} is below one; this implies that a daily temperature excursion at the MGR indoor surface higher than at the GrR surface often occurs in days when, however, the indoor roof surface of the GrR is hotter than that of the MGR. Presence of water into the system, demonstrated by ADWP in the order of few days or not null ARI_5, often leads to very variable, and sometimes over unit, STR_{in}. The 92% of STR_{in} higher than one occurred during the wetter autumn-winter months, when water is likely present into the system and STR_{in} time series is more variable day by day. In very wet periods (i.e., ARI_5>65 mm), STR_{in} tends to assume values around

the unit; this could indicate that, during the wettest periods, the possible occurrence of a significant amount of ponding rainwater onto the GrR for a prolonged time, generates similar conditions in the MGR and the GrR, minimizing the thermal differences between the outdoor roof surfaces and leading to similar indoor roof surface temperatures in the two roofs. On the contrary, for ADWP over 1 month that exclusively occurred during the spring-summer period, and thus under a condition of likely absence of water in the MGR, both the thermal indices are less variable and lower than unit; it is possible then to conclude that dry antecedent conditions leads to more stable thermal indices, less influenced by the external air temperature daily variability and always indicating a clear gain of the MGR compared to GrR in terms of thermal insulation and inertia. At the same time, the lowest values for STR_{in} in the series have been reached only in presence of water (e.g. $STR_{in}<0.85$ only for ADWP< 10 days) and TER_{in} tends to decreases as ARI_5 increases.

Fig. 8 is similar to Fig. 7 and refers to the outdoor STR and TER indices and the API_5 and ATI_5 indices which have been normalized for sake of visualization, the former (API_5*) with respect to the maximum API_5 in the series and the latter (ATI_5*) with respect to mean daily temperature over the reference period.

High values of API_5 are indicative of recent precipitation, causing wet soil moisture conditions in the GL and possible water also into the BL, while on the contrary, dry soil moisture conditions of the GL could occur when API_5 is null and ATI_5 is high, since both conditions favor soil dryness processes. From the figure we can notice how STR_{out} slightly increases with API_5*; thus, the possible presence of water in the GL of the MGR, which prevalently occurs during the winter, could improve its thermal performances, leading to roof surfaces of the MGR hotter than those of the GrR during the coldest season of the year. On the contrary, higher ATI_5 values, typically occurring during the hottest summer months, when API_5 values are frequently null, are characterized by lower variability of the STR_{out}, which is stably lower than one, confirming the outcomes of Fig. 7. TER_{out} index, which always denotes daily temperature excursion at the outdoor MGR significantly lower than at the outdoor GrR, appears increasing with ATI_5* and scarcely sensitive to API_5*, probably because other factors here not considered, such as the solar irradiance, the air humidity and the wind conditions, as well as their daily variability, may play a prominent role compared to the presence of water into the GL in determining the daily temperature excursion at the outdoor roof surfaces. Finally, it worth emphasizing that, differently from the indoor thermal indices shown in Fig. 7, the two outdoor thermal indices of Fig. 8 are concordant, with TER_{out} increasing with STR_{out} and this last always above one in the few cases with TER_{out} above 0.3.

A direct measure of the water present into the system is given by the *Degree of Water Storage*, DWS (Table 1), whose influence on the STR and TER indices is analyzed in Fig. 9. In particular, this index was classified using the following three ranges: "Empty", when DWS = 0%; "Intermediate", when DWS is between 0% and 50%; and "High", when DWS is higher than 50%, and, thus, the mean daily water level (over 5 cm) is close to the maximum weir closure position (7 cm). For this analysis, the available limited sample of "direct records" of DWS was extended with "reconstructed data", assuming an "Empty" BL when ADWP is longer than 30 days and "High" condition of the BL at the days with not null outflow discharge from the MGR.

From the analysis of the outdoor and indoor indices in Fig. 9, it emerges how despite STR indices are scarcely affected from the presence of water into the BL in terms of mean and median values, the dispersion of the values around the mean increase with increasing water storage, leading to some occurrences of STR_{out} and STR_{in} above the unit that imply temperature at the MGR surfaces higher than at GrR surfaces; this is not necessarily a disadvantage in terms of internal comfort, considering that "High" water storage conditions prevalently occurs during the wetter and colder wintry months, when hotter roof surfaces could reduce heating energy demand. Such a behavior could be explained by a gain in terms of thermal inertia due to water storage in the BL that slows down heat dispersion from internal to external environments, which also justifies what can be considered as the most evident impact of the presence of stored water on the thermal response of the MGR, that is the marked reduction of the daily thermal excursion shown in the right plots of Fig. 9. From the figure, it can be observed how passing from "Empty" to "High" conditions, the distribution of both TER_{in} and TER_{out} indices changes markedly, shifting downwards and assuming a positive skew.

4. Discussion

The analyses carried out in the present work have allowed to quantify the thermal performances of a relatively small MGR under a typical semi-arid Mediterranean climate, focusing on the modifications induced on the indoor/outdoor roof surface temperature.

All the analyzed indices are concordant in highlighting an overall

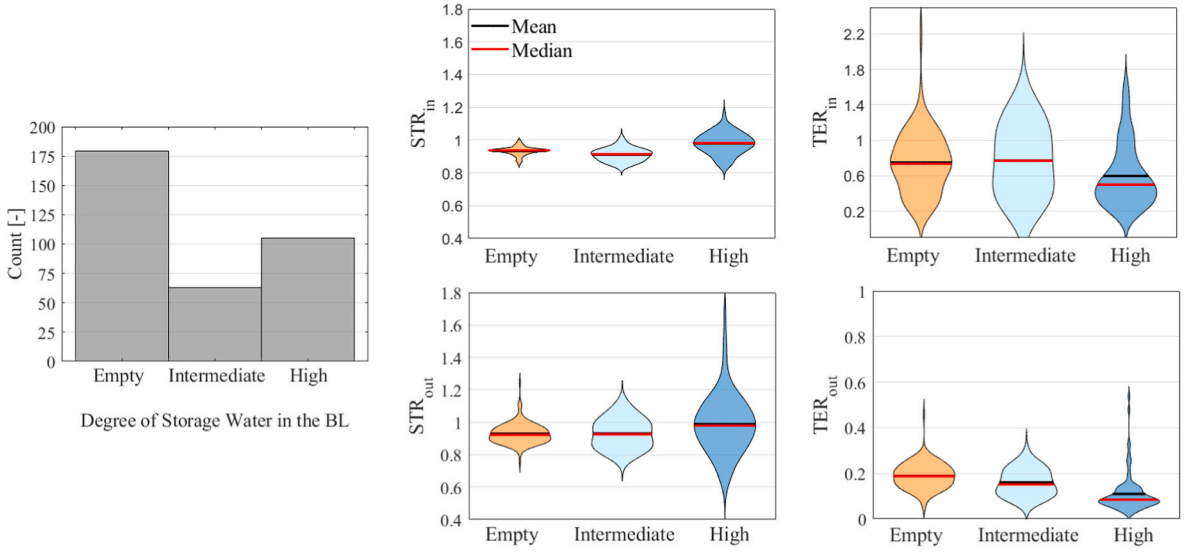

Fig. 9. Frequency histogram (left plot) of the three classes of DWS: Empty (DWS = 0%), Intermediate (0% ≤ DWS ≤50%), High (DWS>50%). Distribution plots (middle and right plots) of the corresponding STR_{in} and TER_{in} (top), and STR_{out} and TER_{out} (bottom), with indication of mean (black lines) and median (red). (For interpretation of the references to color in this figure legend, the reader is referred to the Web version of this article.)

cooling effect (Table 2) for the MGR outdoor surface, especially during the warm periods, and a heat storage effect demonstrated by the increment of the minimum daily temperature, especially in the colder periods, that might favoring an easier reaching and keeping of comfort temperatures in the indoor environments [52]; this aspect, in turn, implies a potential consistent reduction of the yearly energy demand, and the consequent costs, for air-conditioning. Moreover, as it was demonstrated by the daily profiles shown in Fig. 5, the MGR layers mitigate the influence of weather on the outdoor rooftop, with effective protection of roof membrane against both rapid cooling during the cold winters and the influence of intense solar radiation during the hot summers, thus prolonging its lifetime [24].

The mean daily surface temperature of the conventional grey roof was found to be considerably higher than air temperature (on average + 2.6 °C), especially during the summer, and even more relevant differences resulted for the maximum daily temperature (up to +16 °C in the summer); this might influence considerably the microclimate conditions above the roof. Our analysis has demonstrated how the presence of a vegetated roof may significantly reduce the external mean daily roof surface temperature; in our case we observed a reduction over the entire year of almost 2 °C with a reduction of −3 °C during the summer. Vegetation present in the MGR act as an insulation layer by reducing convective heat flow, while soil may act as a thermal resistance and a heat sink; all this is reflected in a considerable lowering of the daily temperature peaks, which in our experimental site reached a mean reduction of about −15 °C during the summer. Moreover, the dominant way for vegetated surfaces to dissipate the absorbed heat is by evapotranspiration [53], which contributes to the reduction of the surface temperature of the materials and the increase of the external air humidity, producing an overall cooling effect for the air surrounding the building [54], which confirms the potential of green roofs to reduce UHI effect [55]. In multilayer GRs, this effect is even more pronounced than in conventional GRs due to the increased water storage that can supply evapotranspiration processes.

The reduction of the outdoor roof surface temperature is also reflected in a lowering of the indoor surface temperature; we observed, on average, a difference of −1.3 °C between the mean daily temperature recorded at the indoor MGR and GrR sensors. Moreover, the analyzed MGR produced a significant reduction of the mean daily temperature excursion compared to the benchmark grey roof, for both outdoor and indoor sensors equal to 86% and 31%, respectively, with maximum percent reduction during the summer equal to 92% and 39% at the outdoor and indoor sensors, respectively; this last reduction, in particular, provides clear insight of a higher thermal insulation capacity and thermal inertia, which can potentially contribute in improving the energy efficiency class of existing buildings.

For a conventional GR installation in Chicago (USA) [56], showed that the roof surface temperature on the hottest day was 22 °C lower than a reference grey rooftop. In semi-arid Mediterranean regions, such as Sicily, the thermal advantages of vegetated roofs during the hotter months are more evident than during the colder season, as it is also confirmed by other studies in climatologically similar zones [33]. [57]; reported, for an installation of GR in France, an outdoor surface temperature reduction up to 30 °C during the summer and, for the same season, an indoor air temperature reduction of 2 °C; in the same study, authors quantified a 6% reduction of the annual building energy demand [50]. analyzed three extensive green roofs in Calabria, southern Italy, using the same performance indices explored in our study. They found for outdoor sensors values of STR_{avg} between 0.70 and 1.1, consistent with our results. In Ref. [50], the reference roof experienced daily temperature excursions higher than the green roof, with TER values for the winter ranging from 0.44 to 0.61 and for the summer ranging from 0.31 to 0.52; here, our system has experienced even lower TER values, around 0.09, demonstrating a higher potential of the MGRs compared to traditional extensive GRs.

The present study represents, to the best of the authors knowledge, the first attempt to assess quantitatively the influence of water storage on the thermal response of a GR, an aspect that assumes particular relevance for the cases of MGR, which have the potential for storing for long times considerable amounts of rainwater. All the analyses that we have performed are concordant in highlighting that the MGR thermal efficiency, especially in terms of daily temperature excursion reduction, increases with water storage, with median TER_{out} for the system with "High" water storage condition of the BL reduced by the 54% compared to the system with an "Empty" BL (bottom-right plot of Fig. 9); this is also coherent with [50]; where the most irrigated green roof among the three compared was that showing the most important excursion reduction and the lowest TER values. Nevertheless, the response of the MGR in presence of significant water storage resulted much more variable than under dry conditions. Water is characterized by an order of measure higher thermal conductivity compared to air, with heat transfers occurring at a higher rate that could determinate, in presence of water, a higher sensitivity of the thermal indices to the external air temperature and solar irradiation, and thus to their daily and seasonal fluctuations; this could explain the higher variability of the performance indices in presence of water, when both the lowest and the highest values for both STR_{in} and TER_{in} indices have be obtained.

Finally, it is worth emphasizing that during the monitoring period we have not applied any operational rules by the SFC system, never opening the control weir. Actually, our results could offer a new perspective for an optimal management of the control weir in a MGR, not only aimed to minimize/prevent/delay system outflow during the intense storms in wet seasons and/or maximize water detention during the driest periods for passive irrigation and/or later water reuses [42,58]. The real time monitoring of climate and water storage into the system could in fact allow for the implementation of automatic procedures to optimize the use of the SFC system also in terms of best thermal efficiency, to reduce energy consumptions for air conditioning during both the coldest and hottest periods, varying conveniently the amount of water stored into the storage layer as a function of the external weather conditions.

5. Conclusion

Climate change and increasing urbanization are posing growing challenges in urban areas for which new paradigms of climate adaptive design, oriented to the criteria of resilience, sustainability, hydraulic and hydrological invariance are urgently needed. New measures defined within the concept of NBSs, represent multi-purpose techniques capable to simultaneously address various future threats in a resource-efficient and adaptable manner, also allowing for urban regeneration and renewal of areas unused or subjected to the combined effect of endogenous and exogenous criticalities.

This study has presented a new and advanced green infrastructure, that is the MGR that, combining the advantages of traditional green roofs with those of rainfall harvesting systems, represents a measure particularly suitable in semi-arid Mediterranean regions, where the climate could generate serious issues for the implementation of traditional green roofs and the marked intermittent nature of rainfall regime requires an efficient management of urban stormwater and water resources. Stored water in MGRs can supply capillary water to the system vegetation itself, preventing water stress and reducing maintenance costs, and it might be also reutilized as grey water, reducing building water demand and potentially mitigating water scarcity problems. In this work we also highlighted as vegetated roofs can be thought as medium of temperature moderation and energy saving in the building sector; the presence of the storage layer in MGRs that may act as a further insulation layer, has the potential to increase roof thermal inertia, improving the mitigation effect with respect to heat waves and UHI that frequently characterize the largest Mediterranean urban areas.

The design of such a kind of solutions is often oriented primarily to an efficient management of stormwater in urban areas, trying to reduce the pressure on existing urban drainage system during intense storms,

and the possibility of grey water recycling. A previous analysis [42] on the hydrological performances of the experimental site of Palermo here tested, in fact, highlighted how MGRs outperform traditional GRs in terms of capacity to retain/detain rainwater, estimating that a large fraction of retained water, equal to about the 70%, could be potentially reused. In this work, it was explored an aspect much less investigated in literature up to now, that is the thermal benefits that MGRs can provide also in consideration of the degree of fullness of the water storage layer. Due to their recent commercialization, thermal efficiency of MGRs in semi-arid environments had never been tested before; thus, a comprehensive evaluation of the full range of benefits that MGRs could provides, supported by observational studies, is essential to support the current policy directions aimed at promoting climate adaptive urban design paradigms.

Our analysis has shown how the MGR of Palermo was able to produce a reduction of the mean daily temperature equal to 8.4% and 5.8% for outdoor and indoor spaces, respectively, with a significant decrement of the daily maxima (up to 38.2% for outdoor spaces) especially during the diurnal hours of the hottest months. All the daily thermal indices showed performances significantly higher than those referring to traditional extensive green roofs with similar thickness and under similar climate conditions [50], also highlighting how the amount of water stored into the storage layer may have a not negligible influence on the thermal response of MGRs. With this regard, a general outcome was that, despite the thermal performances of the MGR in general increase with water storage, especially for what concerns the reduction of the outdoor daily surface temperature excursion, the presence of water into the system may also induce a high instability of thermal indices, whose distribution under wet conditions shows a dispersion larger than that relative to days with empty storage layer and/or dry green layer. This effect probably occurs since the thermal response of the system in presence of water becomes more sensitive to other factors here not explored, such as solar irradiance, wind, and air relative humidity. A more complete understanding of the water influence on thermal response of the MGR probably would require accounting for some climatic variables here ignored and their mutual influence, and to adopt indices defined on finer time-scales.

The reduction of the roof outdoor/indoor surfaces temperature daily excursion due to presence of water into the blue layer provides a clear indication of an augmented thermal inertia due to the installation of a MGR; this effect, coupled with others typical of vegetated roofs, such as shading through foliage and branches, the increase in air humidity and cooling by evapotranspiration, may be also interpreted as an extremely positive outcome in terms of UHI attenuation. Other research directions to further stress the importance of encouraging future analyses on this type of technology include the exploration of other possible co-benefits not analyzed in the present work, such as the reduction of air and water pollution, the attenuation of noise levels, and the increase of buildings' aesthetic value and, consequentially, of their commercial value.

Funding

The present work was funded by the European Union – NextGenerationEU – with grant MUR D.M. 737/2021 – research project "Multilayer Green Roofs: multipurpose nature based solutions towards sustainable and resilient cities".

CRediT authorship contribution statement

Dario Pumo: Writing – review & editing, Writing – original draft, Visualization, Validation, Supervision, Software, Resources, Project administration, Methodology, Investigation, Funding acquisition, Formal analysis, Data curation, Conceptualization. **Francesco Alongi:** Writing – review & editing, Data curation. **Marcella Cannarozzo:** Writing – review & editing. **Leonardo V. Noto:** Writing – review & editing, Supervision, Resources, Investigation, Conceptualization.

Declaration of competing interest

The authors declare that they have no known competing financial interests or personal relationships that could have appeared to influence the work reported in this paper.

Data availability

Data will be made available on request.

Acknowledgments

The experimental prototype was realized within an agreement with Delft University of Technology (Netherlands) as part of the EIT Climate-KIC program (funding received from the European Union Climatic KIC programme with grant number EIT SGA 2018 supporting project 'Polder Roof Fieldlabs - 180522'). The authors also thank anonymous reviewers and editor-in-chief for their suggestions on the quality improvement of the present paper.

References

[1] C. Milesi, G. Churkina, Measuring and monitoring urban impacts on climate change from space, Rem. Sens. 12 (21) (2020) 3494, https://doi.org/10.3390/rs12213494.
[2] D. Pumo, E. Arnone, A. Francipane, D. Caracciolo, L.V. Noto, Potential implications of climate change and urbanization on watershed hydrology, J. Hydrol. 554 (2017) 80–99, https://doi.org/10.1016/j.jhydrol.2017.09.002.
[3] E. Arnone, D. Pumo, A. Francipane, G. La Loggia, L.V. Noto, The role of urban growth, climate change and their interplay in altering runoff extremes, Hydrol. Process. (2018), https://doi.org/10.1002/hyp.13141.
[4] N.W. Arnell, S.N. Gosling, The impacts of climate change on river flood risk at the global scale, Climatic Change 134 (3) (2016) 387–401.
[5] I.B. Karlsson, T.O. Sonnenborg, J.C. Refsgaard, D. Trolle, C.D. Børgesen, J. E. Olesen, E. Jeppesen, K.H. Jensen, Combined effects of climate models, hydrological model structures and land use scenarios on hydrological impacts of climate change, J. Hydrol. 535 (2016) 301–317, https://doi.org/10.1016/j.jhydrol.2016.01.069.
[6] UN, United Nations Final Report on World Urbanization Prospects 2018, 2018.
[7] M. Swilling, M. Hajer, T. Baynes, J. Bergesen, F. Labbé, J. Musango, A. Ramaswami, B. Robinson, S. Salat, S. Suh, et al., The Weight of Cities: Resource Requirements of Future Urbanization; A Report by the International Resource Panel, United Nations Environment Programme, Nairobi, Kenya, 2018.
[8] M. Santamouris, Recent progress on urban overheating and heat island research. Integrated assessment of the energy, environmental, vulnerability and health impact. Synergies with the global climate change, Energy Build. 207 (2020), 109482, https://doi.org/10.1016/j.enbuild.2019.109482.
[9] F. Estrada, W.W.J. Botzen, R.S.J. Tol, A global economic assessment of city policies to reduce climate change impacts, Nat. Clim. Change 7 (6) (2017) 403–406, https://doi.org/10.1038/NCLIMATE3301.
[10] C. Sarrat, A. Lemonsu, V. Masson, D. Guedalia, Impact of urban heat island on regional atmospheric pollution, Atmos. Environ. 40 (2006) 1743–1758.
[11] C. Cao, X. Lee, S. Liu, N. Schultz, W. Xiao, M. Zhang, L. Zhao, Urban heat islands in China enhanced by haze pollution, Nat. Commun. 7 (2016), 12509.
[12] J. Liu, D. Niyogi, Meta-analysis of urbanization impact on rainfall modification, Sci. Rep. 9 (2019) 7301.
[13] D. Pumo, L.V. Noto, Exploring the linkage between dew point temperature and precipitation extremes: a multi-time-scale analysis on a semi-arid Mediterranean region, Atmos. Res. 105508 (2021), https://doi.org/10.1016/j.atmosres.2021.105508. ISSN 0169-8095.
[14] L. Ruangpan, Z. Vojinovic, S. Di Sabatino, L.S. Leo, V. Capobianco, A.M.P. Oen, M. E. McClain, E. Lopez-Gunn, Nature-based solutions for hydro-meteorological risk reduction: a state-of-the-art review of the research area, Nat. Hazards Earth Syst. Sci. 20 (2020) 243–270, https://doi.org/10.5194/nhess-20-243-2020.
[15] N. Seddon, A. Smith, P. Smith, I. Key, A. Chausson, C. Girardin, J. House, S. Srivastava, B. Turner, Getting the message right on nature-based solutions to climate change, Global Change Biol. 27 (2021) 1518–1546, https://doi.org/10.1111/gcb.15513.
[16] C.M. Raymond, N. Frantzeskaki, N. Kabisch, P. Berry, M. Breil, M.R. Nita, D. Geneletti, C.A. Calfapietra, A framework for assessing and implementing the co-benefits of nature-based solutions in urban areas, Environ. Sci. Pol. 77 (2017) 15–24, https://doi.org/10.1016/j.envsci.2017.07.008.
[17] UN General Assembly, Transforming Our World : the 2030 Agenda for Sustainable Development, 2015, 21 October 2015, A/RES/70/1 available at: https://www.refworld.org/docid/57b6e3e44.html. (Accessed 3 May 2023).
[18] E. Cristiano, R. Deidda, F. Viola, The role of green roofs in urban Water-Energy-Food-Ecosystem nexus: a review, Sci. Total Environ. 756 (2021), 143876.
[19] G. Mihalakakou, M. Souliotis, M. Papadaki, P. Menounou, P. Dimopoulos, D. Kolokotsa, J.A. Paravantis, S. Papaefthimiou, Green roofs as a nature-based

solution for improving urban sustainability: progress and perspectives, Renew. Sustain. Energy Rev. 180 (2023), 113306, https://doi.org/10.1016/j.rser.2023.113306 art.
[20] G. Ercolani, E.A. Chiaradia, C. Gandolfi, F. Castelli, D. Masseroni, Evaluating performances of green roofs for stormwater runoff mitigation in a high flood risk urban catchment, J. Hydrol. 566 (2018) 830–845, https://doi.org/10.1016/j.jhydrol.2018.09.050.
[21] K.L. Getter, D.B. Rowe, J.A. Andresen, S.I. Wichman, Seasonal heat flux properties of an extensive green roof in a Midwestern U.S. climate, Energy Build. 43 (2011) 3548–3557, https://doi.org/10.1016/j.enbuild.2011.09.018.
[22] D. Suszanowicz, A. Kolasa Więcek, The impact of green roofs on the parameters of the environment in urban areas—review, Atmosphere 10 (2019) 792, https://doi.org/10.3390/atmos10120792.
[23] J. Yang, Q. Yu, P. Gong, Quantifying air pollution removal by green roofs in Chicago, Atmos. Environ. 42 (31) (2008) 7266–7273, https://doi.org/10.1016/j.atmosenv.2008.07.003.
[24] M.G. Rasul, L.K.R. Arutla, Environmental impact assessment of green roofs using life cycle assessment, Energy Rep. 6 (1) (2020) 503–508, https://doi.org/10.1016/j.egyr.2019.09.015.
[25] K. Vijayaraghavan, Green roofs: a critical review on the role of components, benefits, limitations and trends, Renew. Sustain. Energy Rev. 57 (2016) 740–752.
[26] M. Hanzl, Urban Forms and Green Infrastructure – the Implications for Public Health during the COVID-19 Pandemic, Cities & Health, 2020, pp. 1–5.
[27] A. Jenkins, Biotic Systems as a Critical Urban Infrastructure during Crisis: Learning from the COVID-19 Pandemic, Cities & Health, 2020, pp. 1–3.
[28] Jing Xie, Shixian Luo, Katsunori Furuya, Dajiang Sun, Urban parks as green buffers during the COVID-19 pandemic, Sustainability 12 (2020) 6751.
[29] U. Berardi, A. GhaffarianHoseini, A. GhaffarianHoseini, State-of-the-art analysis of the environmental benefits of green roofs, Appl. Energy 115 (2014) 411–428.
[30] A. Niachou, K. Papakonstantinou, M. Santamouris, A. Tsangrassoulis, G. Mihalakakou, Analysis of the green roof thermal properties and investigation of its energy performance, Energy Build. 33 (2001) 719–729.
[31] A. Teemusk, Ü. Mander, Greenroof potential to reduce temperature fluctuations of a roof membrane: a case study from Estonia, Build. Environ. 44 (2009) 643–650.
[32] M.A. Polo-Labarrios, S. Quezada-García, H. Sánchez-Mora, M.A. Escobedo-Izquierdo, G. Espinosa-Paredes, Comparison of thermal performance between green roofs and conventional roofs, Case Stud. Therm. Eng. 21 (2020), 100697.
[33] C.M. Silva, M.G. Gomes, M. Silva, Green roofs energy performance in Mediterranean climate, Energy Build. 116 (2016) 318–325.
[34] T.B. Carson, D.E. Marasco, P.J. Culligan, W.R. McGillis, Hydrological performance of extensive green roofs in New York City: observations and multi-year modeling of three full-scale systems, Environ. Res. Lett. 8 (2) (2013), 024036, https://doi.org/10.1088/1748-9326/8/2/024036.
[35] P.A. Versini, D. Ramier, E. Berthier, B. de Gouvello, Assessment of the hydrological impacts of green roof: from building scale to basin scale, J. Hydrol. 524 (2015) 562–575, https://doi.org/10.1016/j.jhydrol.2015.03.020.
[36] G. Krebs, K. Kuoppamäki, T. Kokkonen, H. Koivusalo, Simulation of green roof test bed runoff, Hydrol. Process. 30 (2016) 250–262.
[37] L.V. Noto, G. Cipolla, A. Francipane, D. Pumo, Climate change in the Mediterranean basin (Part I): induced alterations on climate forcings and hydrological processes, Water Resour. Manag. 37 (2023) 2287–2305, https://doi.org/10.1007/s11269-022-03400-0, 2023.
[38] L.V. Noto, G. Cipolla, D. Pumo, A. Francipane, Climate change in the Mediterranean Basin (Part II): a review of challenges and uncertainties in climate change modeling and impact analyses, Water Resour. Manag. 37 (6–7) (2023) 2307–2323, https://doi.org/10.1007/s11269-023-03444-w, 2023.
[39] E. Andenæs, T. Kvande, T.M. Muthanna, J. Lohne, Performance of blue-green roofs in cold climates: a scoping review, Buildings 8 (2018) 55, https://doi.org/10.3390/buildings8040055.
[40] M. Shafique, R. Kim, D. Lee, The potential of green-blue roof to manage storm water in urban areas, Nat. Environ. Pollut. Technol. 15 (2) (2016) 715–718.
[41] D.G. Cirkel, B.R. Voortman, T. van Veen, R.P. Bartholomeus, Evaporation from (Blue-)Green Roofs: assessing the benefits of a storage and capillary irrigation system based on measurements and modeling, Water 10 (9) (2018) 1–21, https://doi.org/10.3390/w10091253.
[42] D. Pumo, A. Francipane, F. Alongi, L.V. Noto, The potential of multilayer green roofs for stormwater management in urban area under semi-arid Mediterranean climate conditions, J. Environ. Manag. 326 (2023), 116643, https://doi.org/10.1016/j.jenvman.2022.116643.
[43] E. Cristiano, A. Annis, C. Apollonio, D. Pumo, S. Urru, F. Viola, R. Deidda, R. Pelorosso, A. Petroselli, F. Tauro, S. Grimaldi, A. Francipane, F. Alongi, L. V. Noto, O. Hoes, F. Klapwijk, B. Schmitt, F. Nardi, Multilayer blue-green roofs as nature-based solutions for water and thermal insulation management, Nord. Hydrol 53 (9) (2022) 1129–1149, https://doi.org/10.2166/nh.2022.201, 2022.
[44] F. Lo Conti, A. Francipane, D. Pumo, L.V. Noto, Exploring single polarization X-band weather radar potentials for local meteorological and hydrological applications, J. Hydrol. 531 (Part 2) (2015) 508–522, https://doi.org/10.1016/j.jhydrol.2015.10.071.
[45] A. Francipane, D. Pumo, M. Sinagra, G. La Loggia, L. Noto, A paradigm of extreme rainfall pluvial floods in complex urban areas: the flood event of 15 July 2020 in Palermo (Italy), Nat. Hazards Earth Syst. Sci. 21 (2021) 2563–2580, https://doi.org/10.5194/nhess-21-2563-2021.
[46] P. Alpert, T. Ben-Gai, A. Baharad, Y. Benjamini, D. Yekutieli, M. Colacino, L. Diodato, C. Ramis, V. Homar, R. Romero, S. Michaelides, A. Manes, The paradoxical increase of Mediterranean extreme daily rainfall in spite of decrease in total values, Geophys. Res. Lett. 29 (2002) 1–31, https://doi.org/10.1029/2001GL013554.
[47] I. Gnecco, C. Berretta, L.G. Lanza, P. La Barbera, Storm water pollution in the urban environment of Genoa, Italy. Atmos. Res. 77 (1–4) (2005) 60–73, https://doi.org/10.1016/j.atmosres.2004.10.017.
[48] H. Kasmin, V.R. Stovin, E.A. Hathway, Towards a generic rainfall-runoff model for green roofs, Water Sci. Technol. 62 (4) (2010) 898–905, https://doi.org/10.2166/wst.2010.352.
[49] M. Razzaghmanesh, S. Beecham, The hydrological behaviour of extensive and intensive green roofs in a dry climate, Sci. Total Environ. 499 (2014) 284, https://doi.org/10.1016/j.scitotenv.2014.08.046, 269.
[50] P. Bevilacqua, D. Mazzeo, R. Bruno, N. Arcuri, Surface temperature analysis of an extensive green roof for the mitigation of urban heat island in southern mediterranean climate, Energy Build. 150 (2017) 318–327, https://doi.org/10.1016/j.enbuild.2017.05.081. ISSN 0378-7788.
[51] G. Mutani, V. Todeschi, The effects of green roofs on outdoor thermal comfort, urban heat island mitigation and energy savings, Atmosphere 11 (2) (2020) 123, https://doi.org/10.3390/atmos11020123.
[52] L. Pastore, R. Corrao, P.K. Heiselberg, The effects of vegetation on indoor thermal comfort: the application of a multi-scale simulation methodology on a residential neighborhood renovation case study, Energy Build. 146 (2017) 1–11, https://doi.org/10.1016/j.enbuild.2017.04.022.
[53] R.M. Lazzarin, F. Castellotti, F. Busato, Experimental measurements and numerical modeling on a green roof, Energy Build. 37 (2005) 1260–1267.
[54] B. Barozzi, A. Bellazzi, M.C. Pollastro, The energy impact in buildings of vegetative solutions for extensive green roofs in temperate climates, Buildings 6 (2016) 33, https://doi.org/10.3390/buildings6030033.
[55] A. Solcerova, F. van de Ven, M. Wang, M. Rijsdijk, N. van de Giesen, Do green roofs cool the air? Build. Environ. 111 (2017) 249–255, https://doi.org/10.1016/j.buildenv.2016.10.021.
[56] J. Sonne, Evaluating green roof energy performance, ASHRAE J. 48 (2006) 59.
[57] I. Jaffal, S.-E. Ouldboukhitine, R. Belarbi, A comprehensive study of the impact of green roofs on building energy performance, Renew. Energy 43 (2012) 157–164.
[58] T. Busker, H. de Moel, T. Haer, M. Schmeits, B. van den Hurk, K. Myers, et al., Blue-green roofs with forecast-based operation to reduce the impact of weather extremes, J. Environ. Manag. 301 (2022), 113750.